Acta Tropica 129 (2014) 52–60

Contents lists available at ScienceDirect

Acta Tropica

journal homepage: www.elsevier.com/locate/actatropica

The periodicity of *Plasmodium vivax* and *Plasmodium falciparum* in Venezuela

María-Eugenia Grillet[a,*], Mayida El Souki[a], Francisco Laguna[a], José Rafael León[b]

[a] *Laboratorio de Biología de Vectores y Parásitos, Instituto de Zoología y Ecología Tropical, Facultad de Ciencias, Universidad Central de Venezuela, Apartado Postal 47072, Caracas 1041-A, Venezuela*
[b] *Escuela de Matemáticas, Facultad de Ciencias, Universidad Central de Venezuela, Apartado Postal 47072, Caracas 1041-A, Venezuela*

ARTICLE INFO

Article history:
Received 1 November 2012
Received in revised form
27 September 2013
Accepted 4 October 2013
Available online 19 October 2013

Keywords:
Plasmodium dynamics
Malaria epidemiology
Wavelet analyses
Rainfall
ENSO
Venezuela

ABSTRACT

We investigated the periodicity of *Plasmodium vivax* and *P. falciparum* incidence in time-series of malaria data (1990–2010) from three endemic regions in Venezuela. In particular, we determined whether disease epidemics were related to local climate variability and regional climate anomalies such as the El Niño Southern Oscillation (ENSO). Malaria periodicity was found to exhibit unique features in each studied region. Significant multi-annual cycles of 2- to about 6-year periods were identified. The inter-annual variability of malaria cases was coherent with that of SSTs (ENSO), mainly at temporal scales within the 3–6 year periods. Additionally, malaria cases were intensified approximately 1 year after an El Niño event, a pattern that highlights the role of climate inter-annual variability in the epidemic patterns. Rainfall mediated the effect of ENSO on malaria locally. Particularly, rains from the last phase of the season had a critical role in the temporal dynamics of *Plasmodium*. The malaria–climate relationship was complex and transient, varying in strength with the region and species. By identifying temporal cycles of malaria we have made a first step in predicting high-risk years in Venezuela. Our findings emphasize the importance of analyzing high-resolution spatial–temporal data to better understand malaria transmission dynamics.

1. Introduction

Malaria, one of the most serious parasitic diseases of tropical ecosystems, is caused by parasites of the genus *Plasmodium* (Apicomplexa: Plasmodidae) and transmitted among human hosts by the bites of infected female *Anopheles* mosquitoes (Diptera: Culicidae). In 2010, malaria was responsible for 219 million cases, causing nearly 700,000 deaths (WHO, 2012). Epidemiologic patterns of malaria can be highly heterogeneous and caused by a complex set of interactions among parasites, vectors, and hosts occurring at specific locations, and at specific times. In low endemic and epidemic areas, *Plasmodium* incidence exhibits regular seasonal cycles and multiyear oscillations over time (Hay et al., 2000). Annual changes in rainfall and temperature may directly or indirectly affect *Anopheles* reproduction and mortality rates, the blood feeding frequency of the mosquito female and the extrinsic incubation period of *Plasmodium* and thereby cause seasonal variations in both vectors and parasites (Stresman, 2010). Longer-term or inter-annual cycles of the parasite might be driven by extrinsic climatic factors (Bouma and Dye, 1997; Bouma et al., 1997; Poveda et al., 2001), intrinsic mechanisms associated with epidemiological dynamics such as host immunity (Hay et al., 2000), or both factors (e.g., Pascual et al., 2008).

In the Americas, malaria is still a serious health concern, with almost 20% of the total population at some degree of risk, especially in countries such as Venezuela, where the reported morbidity has increased significantly in the last decade (WHO, 2012). In Venezuela, *Plasmodium vivax* malaria accounts for 82% of all cases, followed by *P. falciparum* (16%), *P. malariae* (<1%) and *P. vivax*/*P. falciparum* mixed (1.4%) infections (Cáceres, 2011). The pattern of malaria transmission varies regionally, depending on climate, biogeography, ecology, and anthropogenic activities. Whereas *P. falciparum* malaria occurs mostly in the lowland rain forests of the Venezuelan Guayana region, *P. vivax* malaria is endemic in the coastal plains and savannas as well as the lowland Guayana forests (Rubio-Palis and Zimmerman, 1997). Before the successful malaria eradication campaign in the early 20th century in Venezuela, recurrent epidemics occurred every five years, particularly in the savannas landscapes and coastal plains where *Anopheles darlingi* was the main vector of *P. falciparum* (Gabaldon, 1949). This author observed that malaria cycles apparently coincided with periodic fluctuations of the vector population. Later, Bouma and Dye (1997) associated these epidemics of malaria with the El Niño Southern Oscillation (ENSO). This previous work analyzed malaria at the

* Corresponding author. Tel.: +58 2126051404; fax: +58 2126051204.
E-mail address: maria.grillet@ciens.ucv.ve (M.-E. Grillet).

0001-706X/$ – see front matter © 2013 Elsevier B.V. All rights reserved.
http://dx.doi.org/10.1016/j.actatropica.2013.10.007

country level, yearly timescales, and overall malaria incidence (*P. vivax* + *P. falciparum*). However, no study has addressed temporal patterns in malaria infections, specially their inter-annual cycles, by resolving the species and the malaria eco-regions of Venezuela. Such downscaling in space and parasite taxonomy could reveal significant heterogeneity in malaria periodicity. Since malaria has become again a serious health problem in this country (Cáceres, 2011), year-to-year variation in the size of epidemics, are of particular concern. Understanding this inter-annual variability in the population dynamics of malaria can provide useful insights for malaria elimination programs. Furthermore, a better knowledge of the malaria temporal patterns would allow the development of more effective surveillance and early warning systems to predict disease risk in response to changes in climate.

In this paper, we re-examine the question of malaria's multi-year cycles in Venezuela by using primarily a statistical method of time-series analysis well suited for transient patterns in diseases dynamics and environmental conditions over time (non-stationary patterns). We specifically address the following questions: (i) Is there evidence for particular frequencies in the temporal dynamics of malaria? (ii) Is malaria periodicity species-specific and geographically variable? (iii) Is the inter-annual pattern of malaria in Venezuela associated with climate variability? (iv) If so, does rainfall mediate the effect of ENSO on malaria locally? To do this, we analyze the monthly incidence of *P. vivax* and *P. falciparum* (1990–2010) from three endemic regions of the country. We show that ENSO has played a role in the long-term malaria dynamics during the last 20 years in Venezuela, but that the disease–climate relationship is complex, varying in characteristic periodicities and strength according to region and parasite species.

2. Materials and methods

2.1. Study area

Venezuela is located in the northern coast of South America with a surface area of contrasting landscapes including a northern Caribbean coastal plain and the Venezuelan Guayana in the south (Fig. 1). Malaria is a major public health problem in different endemic–epidemic eco-regions of the country such as the lowland rain forest and savannas of Guayana (<200 m), and the north-eastern coastal plains. Currently, the lowland Venezuelan Guayana is considered a region of high-risk of stable malaria mainly caused by *P. vivax* (~76–84% of cases) and *P. falciparum* (~21–15% of cases), and largely transmitted by *An. darlingi* and *An. marajoara* (Magris et al., 2007; Moreno et al., 2007). *Anopheles darlingi* is mainly a riverine and forest-dwelling species, while *An. marajoara* is a mosquito species associated with wetlands, secondary forests, and human intervention (Moreno et al., 2007). The whole Guayana region covers an extensive area of the country (530,145 km^2), however, the population density is very low and heterogeneously distributed in two administrative areas (Fig. 1): the Amazonas State (0.86 inhabitants per km^2) and the Bolívar State (6.74 inhabitants per km^2). Most of the inhabitants of Amazonas live in the north-western corner of the state (in the Atures and Autana municipalities) and belong to predominantly indigeneous ethnic groups (Metzger et al., 2009). Here, the savanna ecosystem is the dominant landscape of malaria transmission (Rubio-Palis and Zimmerman, 1997) and *An. darlingi* is the main species vector. In Bolívar State, the population at risk is mostly localized in the south-east (e.g., in the Sifontes Municipality), where economic activities are agriculture, gold and diamond mining, and forest exploitation. In this endemic area, the lowland forest ecosystem is the dominant malaria landscape, with *An. darlingi* and *An. marajoara* as the main species vectors (Moreno et al., 2007). In the malaria coastal eco-region (Sucre State), along the Caribbean Sea (Fig. 1), the infection is caused by *P.vivax* and transmitted by *Anopheles aquasalis*. This area is largely composed of mangroves, herbaceous and woody swamps. *Anopheles aquasalis* is mainly associated with brackish and freshwater wetlands (Grillet, 2000). Economic activities of the population are mainly fishing, subsistence agriculture, and tourism.

Semi-annual, annual and inter-annual cycles strongly characterize weather and climate variability in Venezuela (Pulwarty et al., 1992). The large-scale spatial features of rainfall are primarily influenced by the annual location of the Atlantic Inter-tropical Convergence Zone (ITCZ), whereas its local spatial variability is controlled by the mountain ranges, the influence of the atmospheric circulation over the Amazon basin, and the local vegetation and land surface. At the inter-annual scale, the Southern Oscillation is the main forcing mechanism of rainfall variability (Pulwarty et al., 1992). Overall, the April–November season carries 88% of the mean annual rainfall in Venezuela. In the Amazonas studied region, the annual rainfall is around 2300 mm and the rainier months are those from May through August, followed by lower rains during September, October and November (Fig. A.1.a, Supplementary material-SM). Drier months include December–March and the annual mean temperature is around 25–28 °C. In Bolívar State, the malaria region is characterized by an average temperature of 24–26 °C and 1000–1300 mm annual rainfall (Huber, 1995). Here, rains display, in particular, a primary peak from May to August followed by a secondary but lower peak from November to January (Fig. A.1.d, SM). In the malaria coastal eco-region, the annual mean temperature is around 27 °C and the total annual rainfall is close to 1000 mm, with a rainy season from May to November and a dry season from December to April (Fig. A.1.g, SM). Northeastern Venezuelan rainfalls (e.g., the Bolivar and Sucre States) are more directly influenced by the ITCZ than the southwestern Venezuelan rainfalls (e.g., the Amazonas State).

Supplementary material related to this article can be found, in the online version, at http://dx.doi.org/10.1016/j.actatropica.2013.10.007.

2.2. Epidemiological and socio-demographic data

State- and municipality-level cases of *P. vivax* and *P. falciparum* were obtained from the Malaria Control Program database, Venezuelan Ministry of Health. Malaria treatment in the country is exclusively carried out by the public health system which uses artemisinin-based combination therapy (ACT) as the first-line treatment for *P. falciparum*, whereas chloroquine and primaquine are applied for the treatment of *P. vivax*. Local health services are obliged to compile all notifications of malaria on a weekly basis. Symptomatic cases are detected by passive and active surveillance as well as reported according to geographic origin. We analyzed regional monthly records for *P. vivax* and *P. falciparum* incidence from 1990 to 2010 with data aggregated across municipalities by state. For Amazonas State, we pooled the malaria data from the north-western part of the state, and we carried out the same procedure with the incidence data from the south-eastern side of Bolívar State (Fig. 1). Complete time series were not available for the coastal eco-region. Therefore, malaria data were studied from 1998 to 2008 from the Cajigal and Benitez Municipalities (Fig. 1). We calculated malaria incidence rates per 1000 inhabitants (No. of new cases × 1000/population at risk per time) by spatial region and by species (*Plasmodium* species). We assumed that the entire population of the studied area was exposed to the risk of contracting malaria; that is, each person contributed exactly 1 person-time of exposure. The malaria incidence rate was calculated by taking into account the human population growth rate predicted for

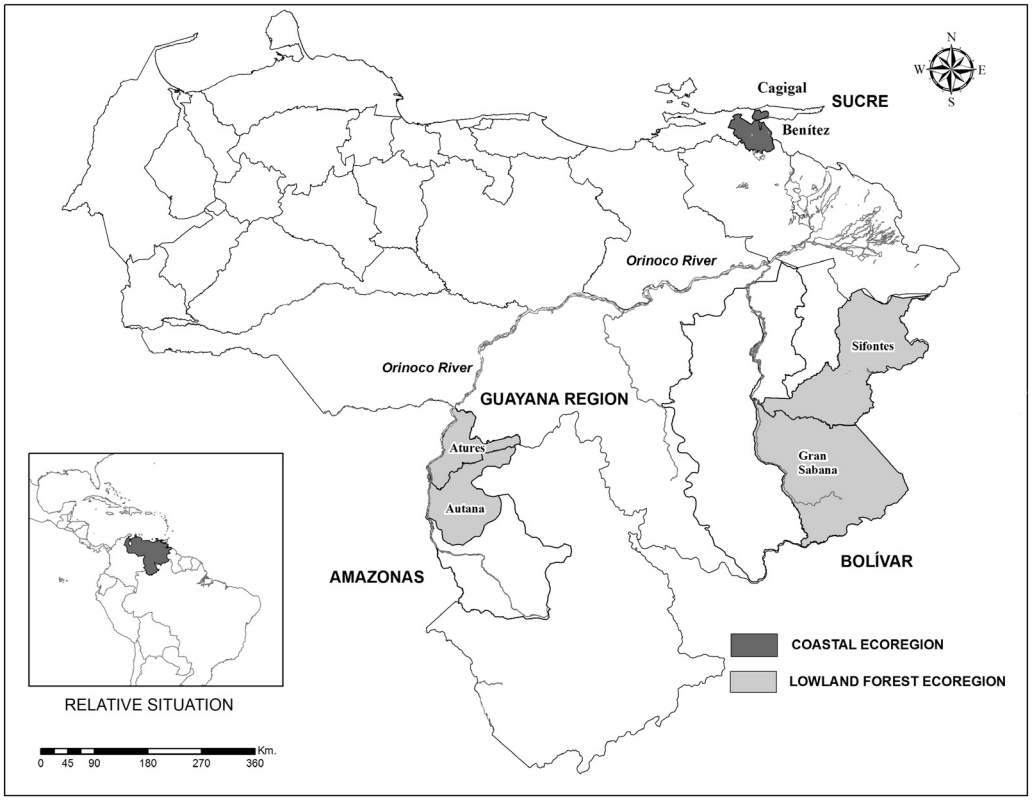

Fig. 1. Map of Venezuela showing the main malaria regions: Amazonas, Bolívar and Sucre States. Malaria cases were aggregated across the municipalities within each state. In the low-land forest eco-region, malaria is caused by *Plasmodium vivax* (84%) and *P. falciparum* (21%), and mainly transmitted by *Anopheles darling*. In the coastal eco-region, the infection is caused by *P. vivax* and transmitted by *An. aquasalis*.

each studied period according to the demographic data (at risk population) from the National Statistics Office of Venezuela.

2.3. Climate data

Contemporaneous meteorological data were obtained from the nearest meteorological stations. The stations by region were: Amazonas (Puerto Ayacucho: 05°39′ N, 67°38′ W); Bolívar (Anacoco: 06°43′ N, 61°08′ W; El Dorado: 06°42′ N, 61°38′ W; Tumeremo: 07°17′ N, 61°30′ W); and Sucre (Guiria: 10°34′ N, 62°17′ W; Irapa: 10°34′ N 62°34′ W; Carupano: 10°39′ N, 63°15′ W). We averaged the data of all stations by each region. Data included mean temperature and rainfall by month; however, we mainly focused on rainfall due to the low annual oscillation of temperature in Venezuela (Huber, 1995). We used the monthly sea surface temperatures (SSTs) of the eastern and central tropical Pacific as an index of the "El Niño" phenomenon (for the Niño Regions known as 3 + 4), the main inter-annual climatic event in the northern coast of South America (Poveda and Mesa, 1997) and Venezuela (Pulwarty et al., 1992). The SST time-series were obtained from the Climate Prediction Center of the National Oceanic and Atmospheric Administration (NOAA, 2011). The atmospheric component linked to El Niño is termed the Southern Oscillation (ENSO) with both atmosphere and ocean phenomena acting together. El Niño corresponds to the warm phase of ENSO, whereas the opposite "La Niña" phase consists of a basin-wide cooling of the tropical Pacific and thus the cold phase of ENSO (Trenberth, 1999). In general, there is a coherent pattern of climatic and hydrological anomalies over the region during extreme phases of ENSO (Poveda and Mesa, 1997). Negative anomalies in rainfall (below-normal), soil moisture and river flows, as well as warmer air temperatures, occur during El Niño for Venezuela (Pulwarty et al., 1992; Poveda and Mesa, 1997). The reverse is true for the cold phase La Niña. El Niño is a climatic oscillation with an average recurrence varying from 2 to 10 years, with an average of about every 4 years (Trenberth, 1999). The events usually include two calendar years, and are generally characterized by SSTs positive anomalies that increase during the Northern hemisphere spring and fall of the first year (Niño^{0}), with the maximum SSTs anomalies occurring during the winter of the following year (Niño^{+1}), and SSTs anomalies receding during the spring and summer of the year $^{+1}$ (Poveda and Mesa, 1997). Six El Niño (1991–1992, 1994–1995, 1997–1998, 2002–2003, 2004, 2009–2010) and three La Niña (1995–1996, 1998–2000, 2007–2008) events occurred during our study period according to the criteria of Trenberth (1999). The 1991–1995 was considered a very long and extended (5-year) El Niño "event", while the 1997–1998 has been one of the strongest El Niño episodes in the last 30 years (Fedorov and Philander, 2000).

2.4. Time series analysis of P. vivax and P. falciparum malaria

Fourier analysis (FA) and the associated Fourier power spectrum has been one of the most common statistical analyses to decompose the variance of a time-series into dominant frequencies, and separate seasonal (annual) from longer-term (multi-annual) cycles. FA is not able however to characterize signals whose frequency content changes with time in a transient manner. Thus FA cannot provide information on when particular frequencies are present (Cazelles et al., 2007). Because, epidemiological and environmental time-series, as well as their associations, can be strongly non-stationary (varying in time), a different spectral method known as wavelet analyses (WA) has been applied to analyze their periodic and dominant components and how they change over time (Cazelles et al., 2007; Torrence and Compo, 1998). Here, WA

was performed using the Morlet wavelet transform which can be regarded as a generalization of the Fourier transform that allows the localization in time of the analyses; by analogy with spectral approaches, one can compute the global power spectrum by averaging the local wavelet spectrum over time (Cazelles et al., 2007). Thus, the wavelet power spectrum (WPS) estimates the distribution of variance between different frequencies at different time locations.

The time-series were first filtered with a low-pass filter to remove the seasonality and focus on their inter-annual variability. Also, data were square-root transformed and normalized. In addition, wavelet coherency (WC) was used to compare the frequency components of the *Plasmodium* and climate time-series in the three regions and quantify the statistical (linear) association between variables locally in time (Cazelles et al., 2007). WC provides local information on when two non-stationary signals are linearly correlated and at what particular frequency.

Finally, the Kulldorff's scan statistics allowed us to identify significant excesses of cases (e.g., the most likely cluster) of *P. vivax* and *P. falciparum* incidence in time (Grillet et al., 2010). The linear relationship of seasonal anomalies in malaria with seasonal anomalies of El Niño and rainfall were explored through cross-correlation functions. We obtained the standardized anomaly by subtracting the long-term mean value (e.g., 1990–2010 period) of a particular season (3-month running mean) and by scaling this anomaly using the seasonal standard deviation. This standardization method filters out the annual cycle in each variable, and highlights changes between years (inter-annual cycles). We performed all the time-series analyses using original algorithms developed in Matlab (V.7.5, The MathWorks, Natick, Massachusetts, United States) by Cazelles et al. (2007). The software SaTScan V.9.0.1 (Kulldorff, 1997) was used for the Kulldorff's Scan analysis.

3. Results

3.1. Temporal patterns of P. vivax and P. falciparum incidence

The temporal pattern of *P. vivax* and *P. falciparum* cases in the three malaria regions of Venezuela is shown in Fig. 2. In general, both parasite species have exhibited a significant rise in incidence in the south-eastern region of Bolívar State. By contrast, disease incidence has gradually declined in the coastal eco-region. Particularly, for the Amazonas State, the annual incidence of *P. vivax* increased from 12 (1998) to 64 (2004) cases per 1000 inhabitants, depicting a significant time clustering of malaria cases (Fig. 2a) during 2001–2008 (Relative Risk: $RR = 2.0$, log-likelihood ratio = 4846, $P < 0.001$). The annual incidence of *P. falciparum* varied from 5 cases per 1000 in 2010 to 25 cases per 1000 during 2004, when a significant epidemic peak was detected (Fig. 2a; $RR = 2.2$, log-likelihood ratio = 1073, $P < 0.001$). In the Bolívar State, cases of *P. vivax* (Fig. 2b) ranged from 1 case (1993) to 29 cases per 1000 in 2010, showing a significant and positive trend from 2003 onwards (linear model, $R^2 = 0.77$, $P < 0.05$), and an epidemic period from 2004 to 2010 ($RR = 4.2$, log-likelihood ratio = 51,243, $P < 0.001$). Similarly, *P. falciparum* cases had a significant positive trend during the study period (linear model, $R^2 = 0.77$, $P < 0.05$) and an epidemic peak during 2010 (Fig. 2b), when the annual incidence rate reached 10 cases per 1000 ($RR = 5.1$, log-likelihood ratio = 11,860, $P < 0.001$). In the northern Sucre State (Fig. 2c), *P. vivax* showed an epidemic peak during 2002 (18 cases per 1000 inhabitants, $RR = 4.5$, log-likelihood ratio = 8579, $P < 0.001$), although malaria infection has displayed a significant negative trend (linear model, $R^2 = 0.67$, $P < 0.05$) during the last years.

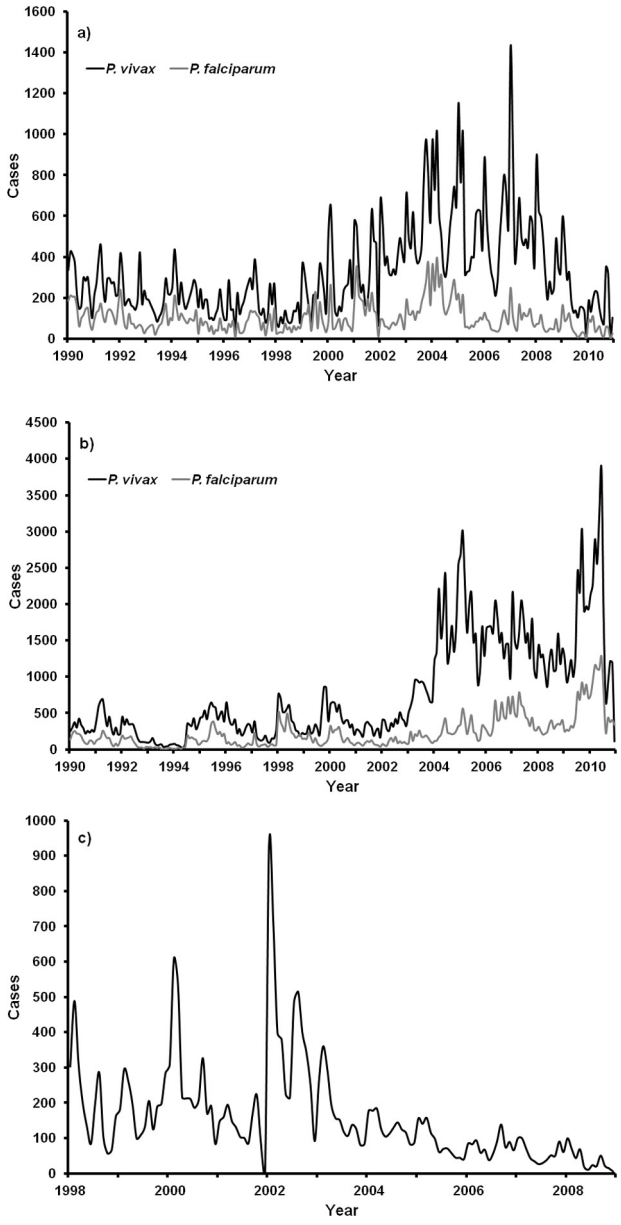

Fig. 2. Monthly time series of malaria cases in (a) Amazonas, (b) Bolívar, and (c) Sucre regions.

3.2. Periodicity of malaria, ENSO and rainfall

Overall, multi-annuals oscillations of *Plasmodium* at the 2-year and 3–6-year bands were detected and dominated the malaria dynamics in the three regions. However, these parasite cycles were transient and varied in time and space. The global spectrum of *P. vivax* time-series in the Amazonas State showed (Fig. 3a, right panel) a significant and dominant period of 4-year. Locally in time, the wavelet power spectrum-WPS (Fig. 3a, left panel) revealed that this oscillatory mode was most pronounced after 2002 and that a weaker 2-year period was detected in the late 1990s. A similar pattern was found for *P. falciparum* cases after 1999, except that the longer cycle had a greater amplitude (Fig. 3b, right panel), and the shorter one had a stronger signal (Fig. 3b, left panel). In Fig. 3c, the periodicity of ENSO is depicted. The SST time-series exhibited inter-annual variability for the 3–6 and 2-years bands, but the first cycle had higher power, variance and significance from the end of 1990s and the beginning of the 2000s (Fig. 3c, left panel), coinciding with

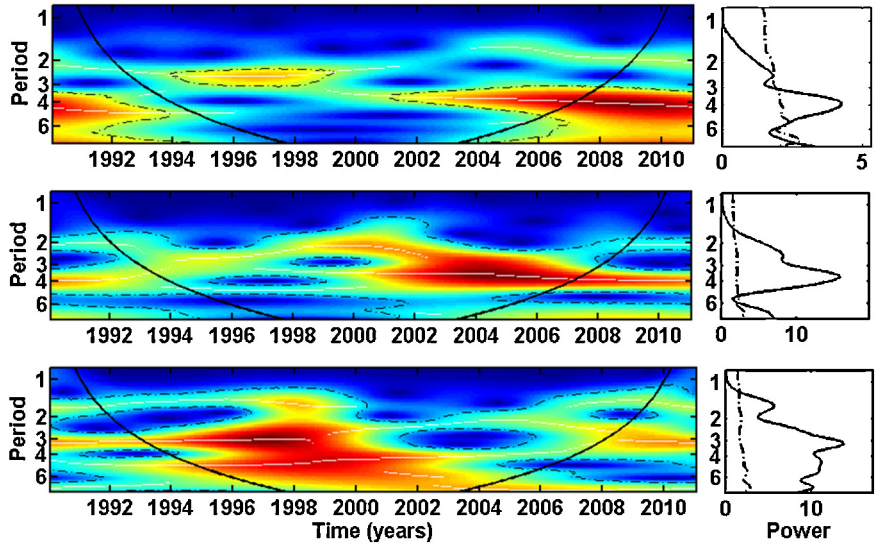

Fig. 3. Patterns of inter-annual variability of the monthly malaria cases of Amazonas region (a (top): *Plasmodium vivax*, b (center): *P. falciparum*) and monthly sea surface temperatures (c (bottom): SSTS). Left: Wavelet power spectrum (WPS). Right: Global spectrum (GS). The *y*-axis describes period (in years), the *x*-axis (GS) describes the power at a given frequency (continuous line) with its significant threshold value of 5% (dashed line). In the WPS, the color code for power values ranges from dark blue, for low values, to dark red, for high ones. The dotted-dashed lines show the $\alpha = 5\%$ significant levels (see Cazelles et al., 2007). The cone of influence (continuous line) in the WPS indicates the region not influenced by edge effects. To remove seasonality, variables were filtered with a low-pass filter. Different scales (years) are used due to the different extent of the time series. (For interpretation of the references to color in this figure legend, the reader is referred to the web version of this article.)

the 3 Niño events of that period. In the Bolívar region, the *P. vivax* time-series showed a continuous oscillation period of high amplitude around the 3–6-year mode (Fig. 4a). By contrast, a transient multi-annual cycle around the 3-year periodic band was detected for *P. falciparum* incidence (Fig. 4b). For the coastal region, a biennial cycle dominated the *P. vivax* periodicity (Fig. 4c, right panel) but the power of this oscillation mode was most intense before 2005 (Fig. 4c, left panel). Finally, we investigated the patterns of inter-annual variability of rainfall in the three regions (Fig. 5). In general, rainfall spectra exhibited power at periods of 3–6 and 2-years bands. The long-term periodicity of rainfall in the Amazonas region (Fig. 5a) was characterized by two areas of high significance for the 2-year and 5–6-year periodic bands, especially after 1997. By contrast, rainfall in the Bolívar region showed inter-annual variability for the 2–4-year band (Fig. 5b) before 2006, whereas rains in Sucre exhibited one main oscillation around the 2–3-year mode (Fig. 5c).

3.3. Malaria periodicity and ENSO

We evaluated the correspondence of the wavelet spectra for malaria and ENSO through the cross-coherence spectrum (WC). As Fig. 6 shows, there was a significant but transient cross-coherence between both variables across the three regions, especially for the 3–6 year scale. This coupling was most marked with the *Plasmodium* time-series of Bolívar (Fig. 6b and Fig. A.2.b, SM). Additionally, a

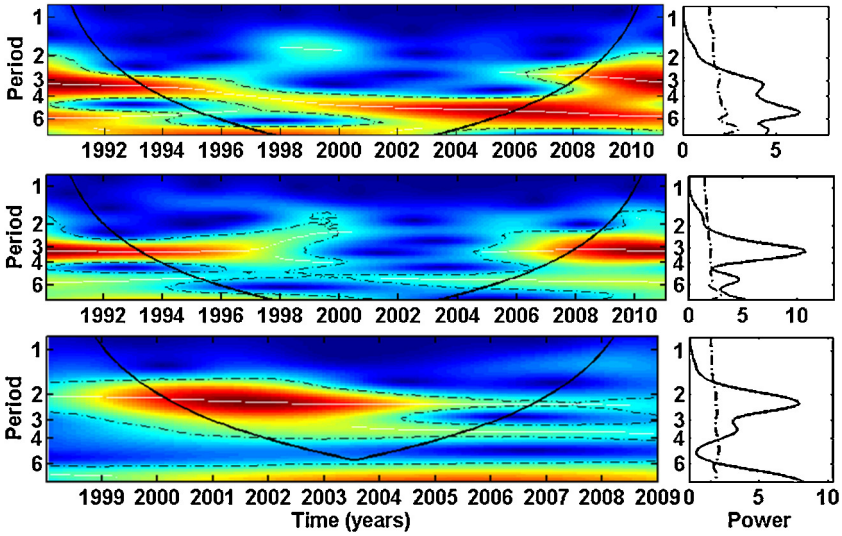

Fig. 4. Patterns of inter-annual variability of the monthly malaria cases of Bolívar (a (top): *Plasmodium vivax*, b (center): *P. falciparum*) and Sucre (c (bottom): *P. vivax*) regions. Left: Wavelet power spectrum (WPS). Right: Global spectrum (GS). The *y*-axis describes period (in years), the *x*-axis (GS) describes the power at a given frequency (continuous line) with its significant threshold value of 5% (dashed line). In the WPS, the color code for power values ranges from dark blue, for low values, to dark red, for high ones. The dotted-dashed lines show the $\alpha = 5\%$ significant levels (see Cazelles et al., 2007). The cone of influence (continuous line) in the WPS indicates the region not influenced by edge effects. To remove seasonality, variables were filtered with a low-pass filter. Different scales (years) are used due to the different extent of the time series. (For interpretation of the references to color in this figure legend, the reader is referred to the web version of this article.)

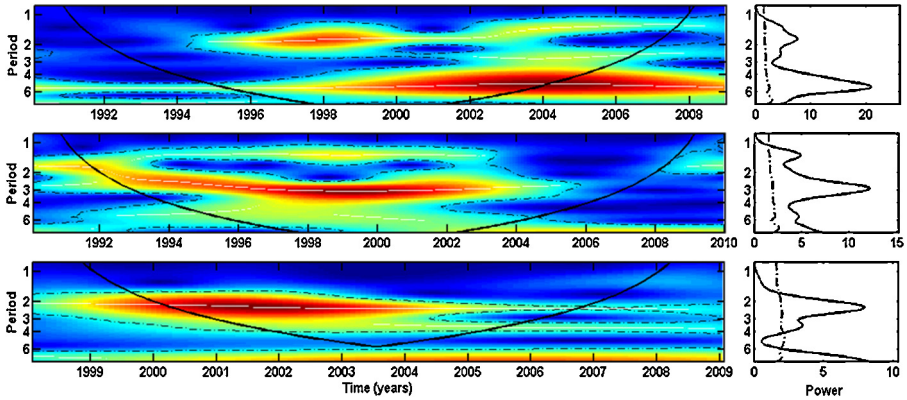

Fig. 5. Patterns of inter-annual variability of the monthly rainfall of Amazonas (a: top), Bolívar (b: center), and Sucre (c: bottom) regions. Left: Wavelet power spectrum (WPS). Right: Global spectrum (GS). The *y*-axis describes period (in years), the *x*-axis (GS) describes the power spectrum (continuous line) with its significant threshold value of 5% (dashed line). In the WPS, the color code for power values ranges from dark blue, for low values, to dark red, for high ones. The dotted-dashed lines show the $\alpha = 5\%$ significant levels (see Cazelles et al., 2007). The cone of influence (continuous line) in the WPS indicates the region not influenced by edge effects. To remove seasonality, variables were filtered with a low-pass filter. Different scales (years) are used due to the different extent of the time series. (For interpretation of the references to color in this figure legend, the reader is referred to the web version of this article.)

weaker cross-coherence between malaria and SST time-series was observed for the 2 year scale, especially for Amazonas (Fig. 6a and Fig. A.2.b, SM) and Sucre (Fig. 6c). The role of ENSO on the malaria temporal dynamics in Bolívar was further supported by the positive correlations we found between the annual *P. vivax* cases and the seasonal SST anomalies from July through September ($r = 0.52$; $P < 0.05$) and October through December ($r = 0.52$; $P < 0.05$) of the previous year. We also observed significant correlations between annual malaria by *P. falciparum* and the seasonal SST anomalies of the previous year (July–September: $r = 0.75$; $P < 0.001$ and October–December: $r = 0.67$; $P < 0.001$). This suggests that number of malaria cases intensifies in the year following an El Niño event in this endemic area. Similarly, a high correspondence between seasonal malaria and seasonal SST anomalies of the 9 previous months ($r = 0.57$; $P < 0.05$) was observed for the coastal eco-region.

Supplementary material related to this article can be found, in the online version, at http://dx.doi.org/10.1016/j.actatropica.2013.10.007.

3.4. Malaria seasonality and rainfall

At the seasonal scale, we explored the role of rainfall as a driver of the annual dynamics of *Plasmodium*. The average seasonal cycle of malaria showed a bimodal pattern in the Amazonas and Sucre regions (Fig. A.1.b, c and h, SM): a large peak in January–February (dry season) and a smaller peak in October–November. Rainfall in both regions displays a main season, with their maximum levels varying in time and amplitude (Fig. A.1.a and g, SM). We correlated accumulated rains for different windows during the year with accumulated *Plasmodium* cases separately for the two malaria peaks to find the "rainfall window" with the strongest association to cases in a given malaria season. Rainfalls from October to December had the best correlation with the main peak of malaria in the Amazonas region (*P. vivax*, $r = 0.55$; *P. falciparum*, $r = 0.57$; $P < 0.05$). Additionally, the observed cases of malaria from October to November were significantly associated with the first malaria peak of January–February (*P. vivax*: $r = 0.89$, *P. falciparum*: $r = 0.47$; $P < 0.05$), and the rains from the wetter months (e.g., the JJA season, Fig. A.1.a, SM) showed a negative association with the second annual peak of malaria (*P. vivax*: $r = -0.54$; *P. falciparum*: $r = -0.50$; $P < 0.05$). Together, these results suggest that the rains from the last phase of the season play a critical role in the annual variation of *Plasmodium* cases, whereas the excess of rains results in less malaria than expected. Comparable results were observed in the Sucre region, where the accumulated rains from October to December (Fig. A.1.g, SM) accounted for the first peak of malaria ($r = 0.68$; $P < 0.05$), whereas malaria cases from August to September were explained by the previous malaria of February ($r = 0.92$; $P < 0.001$). Here, rains of the wetter months (JAS season) did not show a significant effect on *Plasmodium* cases at the end of the year albeit the association was negative ($r = -0.36$; $P > 0.05$). Unlike Amazonas and Sucre, malaria in the Bolívar region had a less marked seasonality

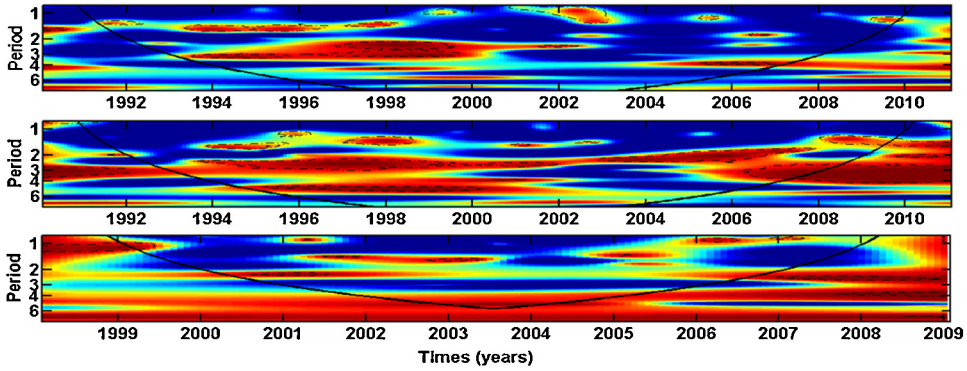

Fig. 6. Wavelet coherence analysis of malaria incidence with the sea surface temperatures (SSTs) time series across three regions: Amazonas (a (top): *Plasmodium vivax*), Bolívar (b (center): *P. falciparum*) and Sucre (c (bottom): *P. vivax*) States. The colors are coded as dark blue, for low coherence and dark red, for high coherence. The dotted-dashed lines show the $\alpha = 5\%$ significant levels (see Cazelles et al., 2007). The cone of influence indicates the region not influenced by edge effects. Different scales (years) are used due to the different extent of the time series. (For interpretation of the references to color in this figure legend, the reader is referred to the web version of this article.)

(Fig. A.1.e and f, SM), especially malaria by *P. vivax*, which showed an almost constant incidence the whole year round. The rainy season in this region is more long and sustained in time compared to the other two regions (Fig. A.1.d, SM) and *P. falciparum* cases seem to exhibit a delayed response to rainfall (Fig. A.1.f, SM). Nevertheless, we found that rains from October to December could account for the cases of *P. vivax* during the January–February period ($r = 0.58$; $P < 0.05$). These lower but sustained rains also explained the malaria by *P. falciparum* from the same period ($r = 0.78$, $P < 0.05$) and from the January–February period ($r = 0.56$, $P < 0.05$). Overall, these results highlight the critical role of the last rains of the season for the annual malaria dynamics in the three studied regions.

3.5. Rainfall and ENSO

At the inter-annual scale, we evaluated the correspondence of the wavelet spectra for rainfall and SSTs. In the Amazonas region, a significant cross-coherence between both variables was found for the 3–6 and 2-years bands (data not shown). Here, the El Niño^{0} event was associated with below-normal rainfall ($r = -0.14$, $P < 0.05$), but interestingly, when we explored different time windows, only the last rains (SON season) had a significant correlation with the seasonal SST anomalies from April through June ($r = -0.45$, $P < 0.05$). Surprisingly, we also observed positive rainfall anomalies during the El Niño^{+1} year, when the event was receding (July–September) or almost gone (October and November). Indeed, the SON accumulated rains during the El Niño^{+1} years were higher compared to those of "neutral" years in this region (*Kruskal–Wallis* test, $H = 4.08$, $P < 0.05$). Particularly, we observed this pattern during the 1992, 1993, 1998, and 2003 years. In the Bolívar region, a significant cross-coherence between rainfall and ENSO was found for the 3–6 year band (data not shown). In this area, the El Niño^{0} years were associated with below-normal rainfall ($r = -0.49$, $P < 0.05$), and the rains from the OND months were also particularly affected by the seasonal SST anomalies from July through September ($r = -0.45$, $P < 0.05$) and October through December ($r = -0.46$, $P < 0.05$). As for the Amazonas region, positive anomalies in the late rainy season of the El Niño^{+1} years (1993, 1994, 1998) generated higher rains compared to those of "neutral" years (*Kruskal–Wallis* test, $H = 5.33$, $P < 0.05$). Finally, rainfall in the Sucre region showed a significant cross-coherence with the SST time-series for the 2 and 5–6 years bands (data not shown). The El Niño^{0} years were associated with below-normal rainfall ($r = -0.24$, $P < 0.05$), and positive rainfall anomalies were also observed at the end of the El Niño^{+1} events but without a significant association.

4. Discussion

In this study, we were able to identify the periodicity of malaria cases by *Plasmodium* species in three malaria endemic regions of Venezuela. The identified cycles in malaria dynamics were transient and differed across regions and species. Cycles within the 3–6-year band dominated the dynamics of the disease in the Guayana region, whereas biennial cycles were dominant in the coastal eco-region, and occasionally, in the Amazonas. Our results partially agree with the previous works of Gabaldon (1949) and Bouma and Dye (1997) on the existence of multi-annual fluctuations in malaria incidence in Venezuela. In particular, Bouma and Dye (1997) described a clear 5-year cycle previous to the 1990s for the coastal zone, where periodicity showed a more regular pattern than in the interior of the country. In contrast, we observed significant heterogeneity for the period 1990–2010 in the malaria periodicity patterns across regions and species, highlighting the importance of analyzing regional spatial–temporal disease data.

Inter-annual epidemic cycles of malaria have been previously detected and accounted for by extrinsic and/or intrinsic factors (e.g., Bouma and Dye, 1997; Chowell et al., 2009; Gagnon et al., 2002; Hay et al., 2000; Pascual et al., 2008; Poveda et al., 2001). Here, we focused mainly on the effects of climatic variability. At the regional scale, ENSO has been the most commonly studied driver of cyclic climate phenomena in human diseases (Kovats et al., 2003). Indeed, we found that the inter-annual variability of malaria cases was coherent with that of SSTs (ENSO), mainly at temporal scales within the 3–6 year bands. These results suggest that climate inter-annual variability has played a role in the multi-annual cycles of malaria in Venezuela for the last 20 years. Although the malaria-ENSO coupling appears more complicated than that reported by Bouma and Dye (1997), we should be cautious when we compare recent associations with previously reported ones (before 1990) given that, first, we are working with different epidemiological settings, and second, ENSO is a quasi-periodic phenomenon whose influence on local weather is not continuous in time, often changing on longer time scales. Indeed, we observed that the effect was most marked during the interval of local maxima of particular El Niño events (1991–1994, 1997–1998). The influence of ENSO on malaria dynamics was further supported by the findings that an increased malaria burden followed elevated SSTs (associated with El Nino conditions) with a delay of 9–12 months. Similar associations were previously reported for Colombia (Bouma et al., 1997; Poveda et al., 2001), India (Bouma and van der Kaay, 1996), and Venezuela (Bouma and Dye, 1997; Gagnon et al., 2002), among others.

Regarding malaria's seasonality in each region, we found two contrasting patterns: bimodal (Amazonas and Sucre) and weak (Bolívar) seasonality. In the first pattern, disease does not seem to follow the observed annual cycle of rains. Main peaks of malaria in Amazonas and Sucre were observed during the dry or transitional periods, whereas rains in both areas were mostly concentrated from May to September–November. Nevertheless, we observed that the minor rains from the last phase of the season play a critical role in the annual variation of *Plasmodium* cases by having a positive influence on the main malaria peak. In contrast, malaria is suppressed in the period with most rainfall, especially in the Amazonas region. Rains promote mosquito breeding sites; but, excessive rainfall can destroy aquatic habitats and flush out the mosquito larvae. In particular, wetlands or large rivers may cause such wash out or become too deep during months with high precipitation. *Anopheles aquasalis*, the malaria vector in the coastal eco-region, is mostly associated to wetlands, and its pre-adult populations are most abundant during the end of the rainy season (October) and at the beginning of the dry season (Grillet, 2000). *Anopheles darlingi*, the main vector in Amazonas (Magris et al., 2007) and Bolívar (Moreno et al., 2007) is most abundant during the least rainy months (October–November; Berti et al., 2008; Moreno et al., 2007), periods when river levels (and therefore, the main aquatic breeding sites) are more stable. Therefore, the ecology of the local vectors can explain why the last rains of the season would be critical for the annual malaria dynamics in given areas. In the Bolívar region, our results revealed, first, that malaria has a delayed response to rainfall, and second, that the minor rains of the season are also critical for *Plasmodium* species dynamics at the beginning of the following year. The almost constant annual disease incidence (especially *P. vivax* malaria) is mainly explained by the differences in seasonal prevalence and relative dominance of species vectors throughout the year. In this region, the mining activity and its associated process of forests clearing creates sustained favorable conditions for the breeding of species such as *An. darlingi and An. marajoara*. Moreno et al. (2007) have shown that the small water-bodies generated by the mining activities are very productive and provide permanent aquatic

habitats for these species during the year, especially *An. marajoara*.

How ENSO drives the long-term periodicity of malaria remains unexplained. The most obvious and plausible pathway for the influence of this regional climatic driver would be through local changes in rainfall and temperature. It would follow that the spatial differences in the malaria cycles among the three studied regions could be understood based on the particular relations of ENSO with the local climate. By analyzing this pathway, we mainly focused on rainfall since it is the main climate variable displaying significant inter-annual variability in Venezuela (Pulwarty et al., 1992) and as we previously showed, the main seasonal driver of the annual dynamics of *Plasmodium*. Rainfall periodicity corresponded to some degree to the observed periodicity in ENSO, but interestingly, each region responded to particular forcing periods. As an example, rains in the Amazonas region exhibited variability around the periods of 2 and 4–6 years, while in the Bolívar region, rainfall mainly showed cycles at the 3-year period. Malaria periodicity corresponded to some degree to that of rainfall. In the Amazonas region, malaria exhibited oscillations of periods 2 and 4, while in the Bolívar region it did at the 3 and 6 periods. Thus, all these results taken together suggest that rainfall mediates the effect of ENSO on malaria locally. In addition, the impact of the El Niño on local rains differed regionally. It was most apparent for the Bolívar region which displayed the higher negative correlations between seasonal rains and SSTs over several time lags. In contrast, Amazonas was the least affected region, by showing lower negative rainfall anomalies during just a few months. What determines whether one particular region responds to a particular forcing period that may not be the strongest is an open question. Some explanations could be found at the regional scale, by exploring the relation between ENSO and the regional rainfall in South-America and Venezuela. Of particular interest is that rainfall is more directly influenced by the Atlantic Inter-tropical Convergence Zone (ITCZ) in Bolívar and Sucre than in the Amazonas (Pulwarty et al., 1992). Although there is an expected coherent pattern of climatic and hydrological anomalies in tropical South-America during phases of ENSO, regional differences in timing, amplitude, sign and intensity of the event have been previously reported within Venezuela (Pulwarty et al., 1992) and Colombia (Poveda et al., 2001). Lastly, the biennial oscillation detected in the malaria series of Sucre and Amazonas opens other questions on the probable influence of the quasi-biennial oscillation (QBO), which is another large-scale ocean-atmospheric phenomenon affecting the hydro-climatology of South-America at inter-annual timescales (Poveda and Mesa, 1997). ENSO itself also exhibits an important quasi-biennial (QB) component, which was detected in our analyses.

How the El Niño and related rainfall patterns affect disease transmission is also a matter of conjecture. We found that during El Niño years, above-normal (positive) SST anomalies were associated with below-normal (negative) rainfall anomalies in the three regions as it was expected based on Poveda and Mesa (1997). Surprisingly, positive seasonal anomalies in rains were also described from July to December in the last phase of El Niño^{+1} year resulting in wetter months compared to similar periods for the non-Niño years. These findings suggest that the impact of the El Niño event on local rains can be complex (with both negative and positive effects). Also, there was a differential impact of ENSO on rains, with an effect mostly at the end of the rainy season. Bouma and Dye (1997) did not observe these post-El Niño anomalous rains in Venezuela, even though Poveda and Mesa (1997) describe the climate conditions under which anomalous rains can develop during the El Niño^{+1} in Venezuela. Some hypotheses can be proposed. As we observed, the last rains of the season were associated with the main peak of malaria at the beginning of the following year. Then, the number of cases in this first outbreak influenced in turn disease burden later in the year. Thus, higher than expected anomalous rains in this phase of the season could increase the size of the main malaria peak, and the number of cases in the following year. Indeed, malaria epidemics were detected several months after these anomalous wetter months. Otherwise, these anomalous rains could promote better breeding conditions for vector populations, and consequently, more malaria cases several months afterwards. As suggested by Gabaldon (1949), larger seasonal abundances of the vectors would explain the interannual cycles of malaria. Future studies should address these hypotheses. In particular, the role of the positive anomalous rains during the El Niño^{+1} event can be elucidated by using a more extensive time-frame (longer malaria and climate series). One alternative conjecture would be that when aquatic habitats are re-established after dry years, mosquito populations can increase to higher than usual numbers because predators of larvae have been reduced (Bouma and Dye, 1997; Grillet et al., 2002). Another hypothesis would invoke additional ENSO-related climate variables such as changes in wind direction (Poveda and Mesa, 1997) which might affect, with a delay of several months, the dispersal and distribution of malaria vectors (Bouma and Dye, 1997). Also, a reduction in transmission during a dry year is likely to reduce population immunity and hence increase the size of the vulnerable population in the following transmission season (Bouma and Dye, 1997). Further research into the ecology of *Anopheles* and *Plasmodium* species are needed to fully understand the causal relationships between ENSO and malaria transmission.

Our results further showed that disease periodicity can be modified by local malaria control measures (Anderson and May (1992). Irregular dynamics in the coastal eco-region were probably affected by the falling of *P. vivax* cases after 2003 as a result of massive control efforts (Cáceres, 2008). Although the similarity in malaria periodicity across regions supports the hypothesis of a regional environmental driver, our findings also indicated differences between *Plasmodium* species. We observed stronger associations between the seasonal malaria peaks for *P. vivax* than for *P. falciparum*, a pattern suggesting a role of relapses, a feature of the life-cycle of the former parasite but not the latter. We also detected irregular dynamics for *P. falciparum* in Bolívar and for *P. vivax* in the Amazonas that we were not able to explain. Finally, the significant upward trend of malaria during the last 10 years in the Bolívar region raises the question of whether this epidemic has contributed to the changes in *P. vivax* periodicity during the study period. Social (mining activities), epidemiological and environmental changes (deforestation) occurring lately in southern Venezuela could explain this malaria growth. Thus, it would be interesting to know if epidemiological and demographic processes account for the different periodicities of malaria cases. Future research should investigate how climate forcing interacts with relapses, host immunity, and demographic and land-use change to determine the population dynamics of the disease in Venezuela.

Conflict of interest

The authors declare they have not competing interests

Acknowledgements

We acknowledge the logistic support provided by the Minister of Health of Venezuela (A. Girón, A. Martinez and M. Herrera), Y. Rangel, J. Moreno, M. Magris, A. Mejía, E. Navarro, O. Noya, A. Zorrilla, F. del Ventura, F. Marichal, N. Moncada and V. Behm. J. Williams, R. Barrera, M. Pascual and two anonymous reviewers made valuable comments on the manuscript. The study was supported by the Venezuelan “Fondo Nacional de Investigaciones

Científicas" (FONACIT, UC-2008000911-3) and the Council for Sciences and Humanities Development (CDCH-PG-0382182011).

References

Anderson, R.M., May, R.M., 1992. Infectious Diseases of Humans: Dynamics and Control. Oxford University Press, Oxford, United Kingdom.

Berti-Moser, J., Gonzales-Rivas, J., Navarro, E., 2008. Fluctuaciones estacionales y temporales de la densidad larvaria de *Anopheles darlingi* root (Diptera: Culicidae) y familias de insectos asociados al hábitat en El Granzón, Parroquia San Isidro, Municipio Sifones del estado Bolívar, Venezuela. Bol. Dir. Malariol. Salud Amb. 48, 177–189.

Bouma, M.J., Dye, C., 1997. Cycles of malaria associated with El Niño in Venezuela. J.A.M.A. 278, 1772–1774.

Bouma, M.J., van der Kaay, H.J., 1996. El Niño Southern Oscillation and the historic malaria epidemics on the Indian subcontinent and Sri-Lanka. Trop. Med. Int. Health. 1, 86–96.

Bouma, M.J., Poveda, G., Rojas, W., Chavasse, D., Quiñones, M., Cox, J., Patz, J., 1997. Predicting high-risk years for malaria in Colombia using parameters of El Niño Southern Oscillation. Trop. Med. Int. Health 2, 1122–1127.

Cáceres, J.L., 2008. Malaria antes y después de la cura radical masiva en el estado Sucre, Venezuela. Bol. Dir. Malariol. San. Amb. 48, 83–90.

Cáceres, J.L., 2011. La malaria en el estado Bolívar, Venezuela: 10 años sin control. Bol. Dir. Malariol. San. Amb. 51, 207–214.

Cazelles, B., Chavez, M., Constantin de Magny, G., Geguan, J.F., Hales, S., 2007. Time-dependent spectral analysis of epidemiological time series with wavelets. J. R. Soc. Interface 4, 625–636.

Chowell, G., Munayco, C.V., Escalante, A.A., McKenzie, E., 2009. The spatial and temporal patterns of falciparum and vivax malaria in Perú: 1994–2006. Mal. J. 8, 1–19.

Fedorov, A.V., Philander, G., 2000. Is El Niño changing? Science 288, 1997–2001.

Gabaldon, A., 1949. The nation-wide campaign against malaria in Venezuela. Trans. R. Soc. Trop. Med. Hyg. 43, 113–164.

Gagnon, A.S., Smoyer-Tomic, K.E., Bush, A., 2002. The El Niño southern oscillation and malaria epidemics in South America. Int. J. Biometeorol. 46, 81–89.

Grillet, M.E., 2000. Environmental factors associated with the spatial and temporal distribution of *Anopheles aquasalis* and *Anopheles oswaldoi* in wetlands of an endemic malaric area in north-eastern Venezuela. J. Med. Entomol. 37, 231–238.

Grillet, M.E., Barrera, R., Martínez, J., Berti, J., Fortin, M.J., 2010. Disentangling the effect of local and global spatial variation on a mosquito-borne infection in a neotropical heterogeneous environment. Am. J. Trop. Med. Hyg. 82, 194–201.

Grillet, M.E., Legendre, P., Borcard, D., 2002. Community structure of Neotropical wetland insects in Northern Venezuela. II. Habitat type and environmental factors. Arch. Hydrobiol. 155, 437–453.

Hay, S.I., Myers, M.F., Burke, D.S., Vaughn, D.W., Endy, T., Ananda, N., Shanks, G.D., Snow, R.W., Rogers, D.J., 2000. Etiology of inter-epidemic periods of mosquito-borne disease. Proc. Natl. Acad. Sci. U. S. A. 97, 9335–9339.

Huber, O., 1995. Geographical and physical features. In: Steyermark, J.A., Berry, P.E., Holst, B.K. (Eds.), Flora of the Venezuelan Guayana, Vol. 1. Missouri Botanical Garden. St. Louis & Timber Press, Oregon, pp. 1–61.

Kovats, R.S., Bouma, M.J., Hajat, S., Worrall, E., Haines, A., 2003. El Niño and health. Lancet 362, 1481–1489.

Kulldorff, M., 1997. A spatial scan statistic. Comm. Stat. Theor. Meth. 26, 1481–1496.

Magris, M., Rubio-Palis, Y., Menares, C., Villegas, L., 2007. Vector bionomics and malaria transmission in the Upper Orinoco River, Southern Venezuela. Mem. Inst. Oswaldo Cruz 102, 303–311.

Metzger, W.G., Giron, A.M., Vivas-Martínez, S., González, J., Charrasco, A.J., Mordmüller, B.G., Magris, M., 2009. A rapid malaria appraisal in the Venezuelan Amazon. Malar. J. 8, 291.

Moreno, J., Rubio-Palis, Y., Paez, E., Perez, E., Sanchez, V., 2007. Abundance, biting behavior and parous rate of anopheline mosquito species in relation to malaria incidence in gold-mining areas in southern Venezuela. Med. Vet. Entomol. 21, 339–349.

NOAA, 2011. National Centers for Environmental Prediction Center (Sea Surface Temperature Historical Archives), http://www.cpc.ncep.noaa.gov/products/analysis_monitoring/ensostuff/ensoyears.shtml (Accessed date: 08/02/2011).

Pascual, M., Cazelles, B., Bouma, M.J., Chaves, L.F., Koelle, K., 2008. Shifting patterns: malaria dynamics and rainfall variability in an African highland. Proc. Biol. Sci. 75, 123–132.

Poveda, G., Mesa, O.J., 1997. Feedbacks between hydrological processes in tropical South America and large-scale ocean-atmospheric phenomena. J. Climate 10, 2690–2702.

Poveda, G., Rojas, W., Quinones, M.L., Velez, I.D., Mantilla, R.I., Ruiz, D., Zuluaga, J.S., Rua, G.L., 2001. Coupling between annual and ENSO timescales in the malaria climate association in Colombia. Environ. Health Perspect. 109, 489–493.

Pulwarty, R.S., Barry, R.G., Riehl, H., 1992. Annual and seasonal patterns of rainfall variability over Venezuela. Erdkunde 46, 273–289.

Rubio-Palis, Y., Zimmerman, R.H., 1997. Ecoregional classification of malaria vectors in the neotropics. J. Med. Entomol. 34, 499–510.

Stresman, G.H., 2010. Beyond temperature and precipitation: ecological risk factors that modify malaria transmission. Acta Trop. 116, 167–172.

Torrence, C., Compo, G.P., 1998. A practical guide to wavelet analysis. Bull. Am. Meteorol. Soc. 79, 61–78.

Trenberth, K.E., 1999. The definition of El Niño. Bull. Amer. Met. Soc. 78, 2771–2777.

World Health Organization, 2012. World Malaria Report 2012. World Health Organization, Geneva.